TEC Gradients and Fluctuations at Low Latitudes Measured with High Data Rate GPS Receivers

Charles S. Carrano, *Atmospheric and Environmental Research Inc., Lexington, MA*
Keith M. Groves, *Air Force Research Laboratory, Space Vehicles Directorate, Hanscom AFB, MA*

BIOGRAPHIES

Dr. Carrano leads the Ionospheric Environments and Impacts Group at Atmospheric and Environmental Research, Inc. His research interests include the effects of the ionosphere on GPS and radar. He designed the real-time ionospheric monitoring software currently used by the dual frequency GPS receivers of the AFRL-SCINDA network. He has a PhD in Aerospace Engineering from The Pennsylvania State University and a BS in Mechanical Engineering from Cornell University.

Dr. Groves is currently a Program Manager in the Space Vehicles Directorate of the Air Force Research Laboratory where he investigates ionospheric scintillation and its impact on satellite-based communication and navigation systems. He has a PhD in Space Physics from MIT and a BS in Physics from Andrews University.

ABSTRACT

Large scale gradients in TEC can degrade the performance of Space Based Augmentation Systems (SBAS) that supply differential corrections of ionospheric delay to GPS users to improve positioning accuracy. These gradients can also complicate the analysis of GPS occultation data, the interpretation of verticalized TEC measurements, and the determination of inter-frequency receiver biases. Small scale TEC fluctuations are commonly associated with the scintillation of trans-ionospheric signals that can impact a variety of communication and navigation systems including GPS. Nevertheless, the spatio-temporal morphology of large scale gradients and small scale fluctuations in TEC have yet to be characterized as functions of local time, magnetic latitude, and solar flux.

In this paper, we characterize large scale gradients and small scale fluctuations in TEC using high data rate dual-frequency GPS receivers maintained by the Air Force Research Laboratory (AFRL). These receivers are distributed throughout the American, Indian, and Asian longitude sectors and primarily in the low latitude regions of the globe. The intent of this work is not to quantify the morphology of TEC variations but instead to present representative environments at low latitudes that may be useful for system design and impacts assessments. A statistical analysis of large scale TEC gradients as a function of magnetic latitude and local time is presented. Small scale TEC fluctuations are quantified in terms of the 60-second standard deviation of the rate of change of TEC, sampled at 10-50 Hz. The high sampling rates make this quantity sensitive to small scale ionospheric structure (roughly 5-25 meter scale-lengths), depending on the ionospheric projection of the satellite velocity vector and the **E**x**B** drift.

Dominant mechanisms for the generation of large scale TEC gradients at low latitudes include the Appleton anomaly, geomagnetic storms, and electron density depletions associated with Equatorial Spread F (ESF). Small scale TEC fluctuations are closely associated with ionospheric structures responsible for the scintillation of UHF and GPS satellite signals.

INTRODUCTION

The AFRL Scintillation Network and Decision Aid (AFRL-SCINDA) is a network of ground-based receivers that monitor trans-ionospheric signals at the VHF and L Band frequencies. It was established by the Air Force Research Laboratory to provide regional specification and

short-term forecasts of scintillation caused by electron density irregularities in the equatorial ionosphere [*Groves et al.*, 1997]. The AFRL-SCINDA network currently includes 16 dual-frequency GPS receivers that record the scintillation intensity index, S_4, Total Electron Content (TEC), and its rate of change, ROTI, using the full temporal resolution of the receiver hardware (between 10-50 Hz depending on the receiver model). The technical details of how these parameters are calculated from the raw amplitude, pseudorange, and phase measurements may be found in Carrano [2007] and Carrano et al. [2006]. These references describe the techniques we use to estimate and remove hardware timing biases associated with the GPS receiver and satellites from the pseudoranges to determine the calibrated (absolute) TEC. A map showing the locations of the AFRL-SCINDA ground stations as of April 2007 is shown in Figure 1. Most of the stations are positioned between the ionization crests of the Appleton anomaly, as these locations experience the strongest global levels of scintillation.

On a regular basis, we generate daily plots of vertical equivalent TEC versus local time at each ground station using a thin shell approximation with an assumed altitude of 350 km for the ionospheric penetration point [*Carrano et al.*, 2006]. The TEC measured along each GPS satellite link is colored according to the magnetic latitude of the ionospheric penetration point (IPP). Plotting in this format facilitates the study of large scale TEC gradients as a function of both local time and magnetic latitude as measured by a stand-alone GPS receiver. The dominant contribution to the diurnal variation in TEC is due to ionization from solar radiation. However, we also observe contributions from a variety of other physical phenomena. For example, readily apparent in the three days shown in Figure 2, are large scale waves commonly associated with magnetic activity, small scale fluctuations associated with ionospheric scintillation, storm-time enhancements and the subsequent rapid recombination, and strong meridional gradients associated with the recovery phase.

One of the most important contributions to large scale gradients in TEC at low latitudes comes from the Appleton anomaly. The Appleton anomaly is produced by the so-called "fountain effect," whereby ionospheric plasma near the geomagnetic equator is driven upward during the day and subsequently falls earthward along magnetic flux tubes to create crests of increased ionization generally located between 10-20 degrees north and south of the geomagnetic equator. The TEC attains its maximum value globally at the crests of the anomaly, and along the sloping sides of the crests meridional gradients in TEC are

Figure 1. Locations of the AFRL-SCINDA ground stations, as of April 2007. Yellow labels indicate stations equipped with a dual-frequency receiver. The solid and dashed curves shows the approximate locations of the geomagnetic equator and the crests of the Appleton anomaly, respectively.

large. The development of the anomaly depends on the zonal electric field, plasma pressure, and neutral winds which are highly dynamic with significant variability on daily, seasonal, and solar cycle time scales [*Henderson*, 2005].

Variations in the strength and location of the Appleton anomaly crests with respect to a low latitude ground station lead to a high degree of TEC variability measured at that station. For example, Figure 3 shows the variation of TEC measured in Taiwan over a three day period in 2007. Note that the diurnal variation in TEC measured by satellites to the geomagnetic north of the station (yellow and red curves) is roughly the same during these three days. On the other hand, the TEC measured by satellites to the geomagnetic south of the station (blue curves) varies by more than a factor of two, from one day to the next, between local noon and a couple hours after sunset. This can be explained by noting that the location of this station (18° N magnetic latitude) is generally north of the Appleton anomaly. On days when the anomaly is well developed and located just to the south of Taiwan (on March 11 and 13, 2007, for example) the TEC in this direction is large. When the anomaly crests are weak and located closer to the magnetic equator, the TEC to the south of the station is nearly the same as overhead or to the north. It is interesting to note that when solar maximum conditions return in 2011-2013, there may be occasions when the anomaly crest moves northward of this station so that the situation is reversed (large TEC would be measured by satellites to the north rather than to the south).

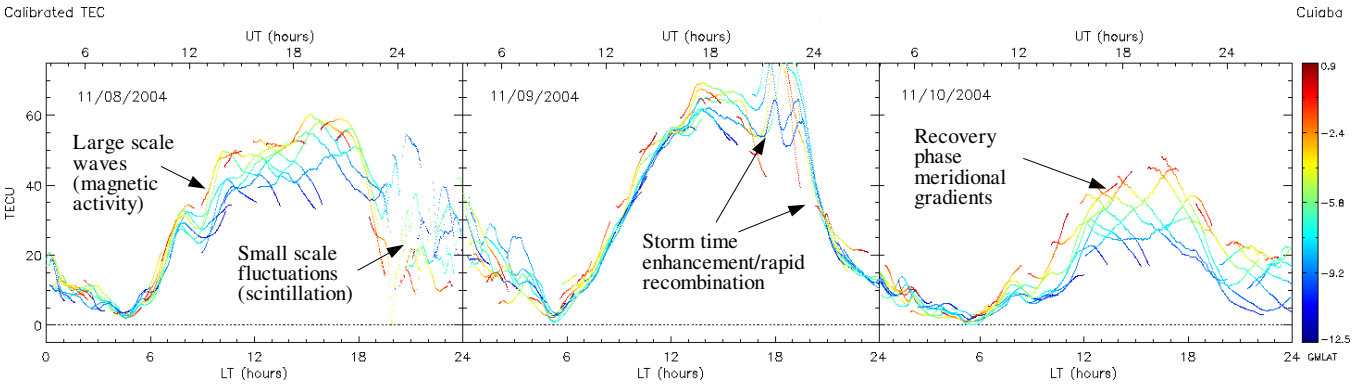

Figure 2. Structural features in the diurnal variation of TEC commonly observed with a GPS receiver operating at low latitudes. The measurements shown were collected at Cuiaba, Brazil (magnetic latitude 6° S) during the three day period November 8-10, 2004.

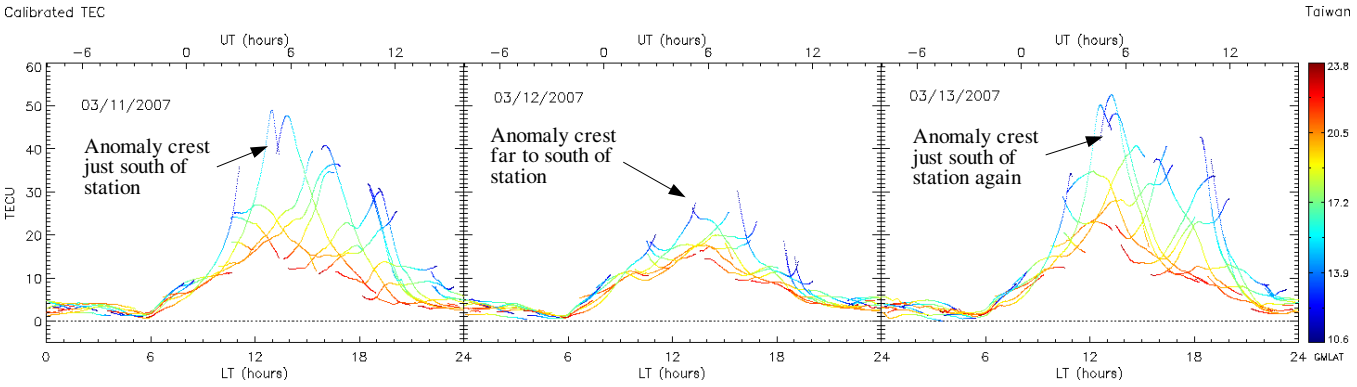

Figure 3. Durinal variation in TEC measured from a ground station near the Appleton anomaly. The measurements of vertical equivalent TEC shown are from Taipei, Taiwan (magnetic latitude 18° N) during the period March 11-13, 2007.

ANNUAL STATISTICS OF TEC

In order to summarize the statistical behavior of large scale gradients in TEC at low latitudes, we computed annual histograms of vertical equivalent TEC as a function of local time at each of the SCINDA ground stations. These histograms are normalized within each local time bin, so that they portray the likelihood (percentage of occurrence) for a given value of TEC to be measured at that time. Only data measured using satellites above 20 degrees in elevation are included in order to minimize errors due to multipath. We chose to produce the histograms on an annual basis since they include a sufficient number of days to provide reasonable statistics while still allowing us to observe the change in these statistics as a function of year within the solar cycle. As an example, Figure 4 shows the annual TEC histogram for Cuiaba, Brazil in 2004.

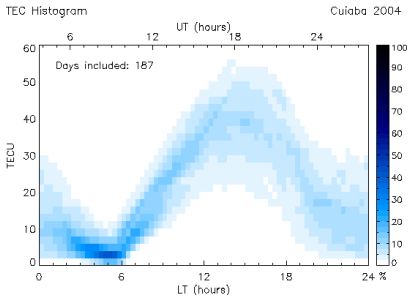

Figure 4. Annual histogram of vertical equivalent TEC as a function of local time at Cuiaba, Brazil (magnetic latitude 6° S) in 2004. The color scale indicates the likelihood for a given value of TEC to be measured at that time.

There are many physical phenomena that contribute to the statistics of TEC in these histograms. The dominant contribution comes from solar radiation, which varies on diurnal, seasonal, and solar cycle time scales. Other contributions include those due to variations in the Appleton anomaly, storm time perturbations, plasma turbulence due to Equatorial Spread F (ESF), and solar flares, among others. While it would seem appropriate to bin the TEC by some parameterization of these effects in order to study their individual contributions to the statistics, it was deemed that there would not be a sufficient number measurements in each bin to provide statistically meaningful results.

A number of structural features in the annual TEC histogram shown in Figure 4 may be readily explained. The ground station lies at 6° S magnetic latitude, or roughly midway between the trough and southern crest of the Appleton anomaly. The large width in the histogram (approximately 25 TECU or 50% of the median TEC value at each local time) between noon and a couple hours after sunset is due largely to variations in the development of the Appleton anomaly. The largest contribution to the statistics from geomagnetic storms also occurs in this local time period. The width of the histogram between sunset and a few hours before dawn is indicative of plasma turbulence caused by ESF which consists of irregularities in the electron density over a wide range of scale sizes. Small scale TEC fluctuations due to ESF frequently result in scintillations in the amplitude and phase of the GPS signal [*Carrano*, 2006]. They are also associated with the scintillations we observe at the VHF frequency by monitoring AF-SATCOM signals from geostationary satellites [*Groves et al.,* 1997]. The width of the TEC histogram in the last few hours preceding sunrise is relatively narrow (no more than 10 TECU) as most of the ionosphere has disappeared by this time through recombination.

The degree of variability in TEC measured at a low latitude ground station depends on the location of the station with respect to the Appleton anomaly. To illustrate the dependence of TEC variability on the magnetic latitude of the observing location, Figure 5a shows annual histograms of TEC collected at Ancon, Peru; Cuiaba, Brazil; Antofagasta, Chile; and Ascension Island. These stations are situated in approximately the same longitude sector (all are in South America except for Ascension Island which lies off the western coast of Africa), but the magnetic latitude of each varies. Figure 5b shows the locations of these stations with respect to a meridional profile of TEC for a typical day in 2005 (close to solar minimum conditions). As can be seen in the figure, both the TEC magnitude and variability (width of the histogram) increase with distance from the magnetic equator for these stations. This occurs because stations farther from the magnetic equator tend to be closer to the Appleton anomaly crests, which are high in density and exhibit substantial variability from day to day and season to season.

a)

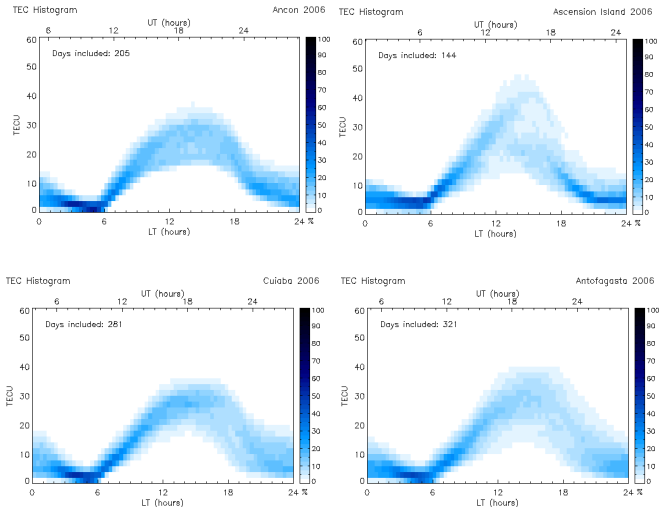

b)

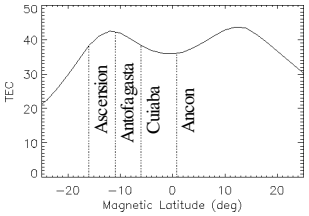

Figure 5. TEC variability as a function of magnetic latitude: a) annual histograms of TEC in 2006 for Ancon, Cuiaba, Antofagasta, and Ascension Island (magnetic latitudes 0°, 6° S, 11° S, and 16° S, respectively), and b) locations of these stations with respect to a typical configuration of the Appleton anomaly.

TEC variability also depends on the average solar flux which is largely controlled by the year within the solar cycle. Figure 6a shows the annual histograms of TEC at Ascension Island during 2004 - 2007, while Figure 6b shows the monthly averaged 10.7 cm solar flux during this period. Note that, on average, both the TEC magnitude and its variability (as characterized by the width of the histogram) decrease as the solar flux decreases. Also readily apparent is a decrease in histogram width between sunset and a few hours before dawn, which occurs because scintillation activity also decreases with average solar flux. At Ascension Island, there are actually two factors involved with the decrease in scintillation activity as solar minimum approaches. First, the intensity of scintillation globally is weaker on average at solar minimum than at solar maximum, and this decrease is quite pronounced at L band frequencies. Second, as solar minimum approaches, the southern crest of the Appleton anomaly moves equatorward, which puts it farther from Ascension Island. Therefore, when scintillation does occur in this longitude sector the irregularities frequently lie too far north of the station to be detected.

a)

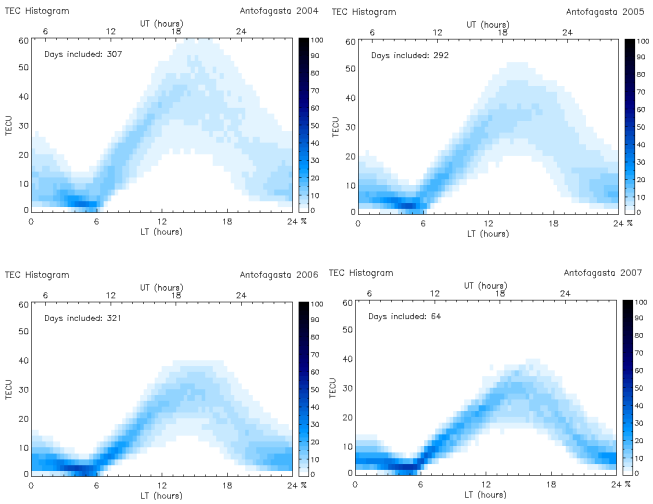

b)

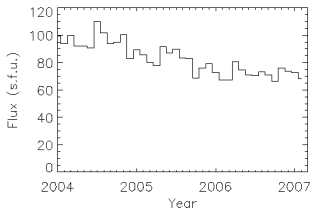

Figure 6. TEC variability as a function of average solar flux: a) annual histograms of TEC for Antofagasta in 2004 - 2007, and b) average solar flux during this period.

TEC FLUCTUATIONS AND SCINTILLATION

The relationship between amplitude scintillations and TEC fluctuations has been explored by a number of authors [*Basu et al.*, 1999; *Beach et al.,* 1999]. In these studies, TEC fluctuations are commonly characterized by the parameter ROTI, defined as the standard deviation (taken over 5 minutes) of the rate of change of TEC, sampled every 30 seconds, i.e.,

$$ROTI^2 = \frac{\langle \Delta TEC^2 \rangle - \langle \Delta TEC \rangle^2}{\Delta t^2} \quad (1)$$

where $<\Delta TEC^2> - <\Delta TEC>^2$ is the variance of the change in TEC between successive samples and Δt is the inverse of the sampling rate. The scintillation intensity index, S_4, is defined as the standard deviation of the signal intensity, I, taken over 60 seconds, normalized by the mean signal intensity over this same interval:

$$S_4^2 = \frac{\langle I^2 \rangle - \langle I \rangle^2}{\langle I \rangle^2} \quad (2)$$

For weak scatter in a power law environment, a relationship between scintillation intensity and TEC fluctuations can be established using phase screen theory [Rino, 1979] and is expressible in the simplified form:

$$S_4^2 \sim \frac{K}{f^2} \langle \Delta N^2 \rangle G' F'(k_N, p_N, f) \quad (3)$$

where K is a constant, f is the frequency, G' is a geometrical factor to account for anisotropy of the magnetic field aligned electron density irregularities, and $<\Delta N^2>$ is the variance of electron density fluctuations along the propagation path. The function F' depends on the frequency, one-dimensional wavenumber, k_N, and spectral slope, p_N, and it vanishes for irregularity scale sizes larger than the Fresnel scale

$$F_r = \sqrt{2\lambda z} \quad (4)$$

where λ is the wavelength and z is the distance from the ground to the screen. Assuming a scattering layer height of 350 km, the Fresnel scale for the GPS L1 wavelength is approximately 365 meters.

Our method for evaluating ROTI is non-standard in that we sample the TEC at the full temporal resolution of the receiver hardware (rather than every 30 seconds), and take the standard deviation of the rate of change of TEC over 60 seconds (rather than over 5 minutes). We will refer to ROTI evaluated in this way as "fast ROTI." The fast ROTI parameter is sensitive to scale sizes on the order

$$d = 2 \Delta t V_r \quad (5)$$

where V_r is the magnitude of the difference between the ionospheric penetration point velocity and the **E**x**B** drift velocity. Assuming a 10 Hz sampling rate and a relative velocity of 120 m/s, the fast ROTI parameter is sensitive to irregularities on the order of 24 meters, which is smaller than the Fresnel scale, and hence to irregularities that can contribute to amplitude scintillations at the L1 frequency. In contrast, the standard definition of ROTI is sensitive to irregularities with scale sizes on the order 7200 meters, which do not contribute to scintillation at the L1 frequency. One might expect the fast ROTI parameter to function as a simple proxy for the scintillation index when the variance of TEC changes between successive samples, $<\Delta TEC^2> - <\Delta TEC>^2$, is a reasonable approximation for the variance in electron density fluctuations along the propagation path, $<\Delta N^2>$, since equations (1) and (3) would then have this term in common.

We calculated annual histograms of fast ROTI and S_4 at each ground station in a similar fashion as for the TEC. The value of the histogram in each local time bin has been normalized to show the percentage occurrence of the value at that time. Only values of fast ROTI above a threshold of 3 TECU/min were included in its histogram to minimize contamination by receiver oscillator noise. Only values of S_4 above a threshold of 0.3 were included in its histogram to minimize the influence of multipath. Since we include only fast ROTI and S_4 data above these thresholds in the histograms, we are implicitly excluding quiet time conditions (when there are no TEC fluctuations or scintillation) from the statistics. To ensure that enough samples are present in each local time bin to yield reliable statistics, we chose to require that there be at least 100 measurements of fast ROTI or 50 measurements of S_4 exceeding their respective thresholds in each local time bin, otherwise no histogram data are shown for that bin.

To observe the statistical behavior of TEC fluctuations and amplitude scintillations at the L1 frequency as a function of solar flux, we computed annual histograms of fast ROTI and S_4 at Antofagasta, Chile for the years 2004 through 2006. These histograms are shown in Figure 7. An Ashtech uZ-CGRS receiver was used to collect these

measurements. The TEC fluctuations parameterized by fast ROTI tend to reach their largest values just after sunset when turbulent production by ESF is strongest, and then they decrease over the course of the night as the turbulence decays. On a statistical basis, both fast ROTI and S_4 exceed their lower thresholds at approximately the same time after local sunset. Similarly, both fast ROTI at S_4 fall below their respective lower thresholds again in the post-midnight sector, on average, as the TEC itself decreases due to recombination. These results suggest that both the onset and duration of TEC fluctuations as parameterized by fast ROTI approximately coincide with amplitude scintillations at L1, at least on a statistical basis and for the cases considered. Both the duration and intensity of the TEC fluctuations and scintillation intensity decrease, on average, as the solar flux decreases (i.e. as conditions approach those of solar minimum).

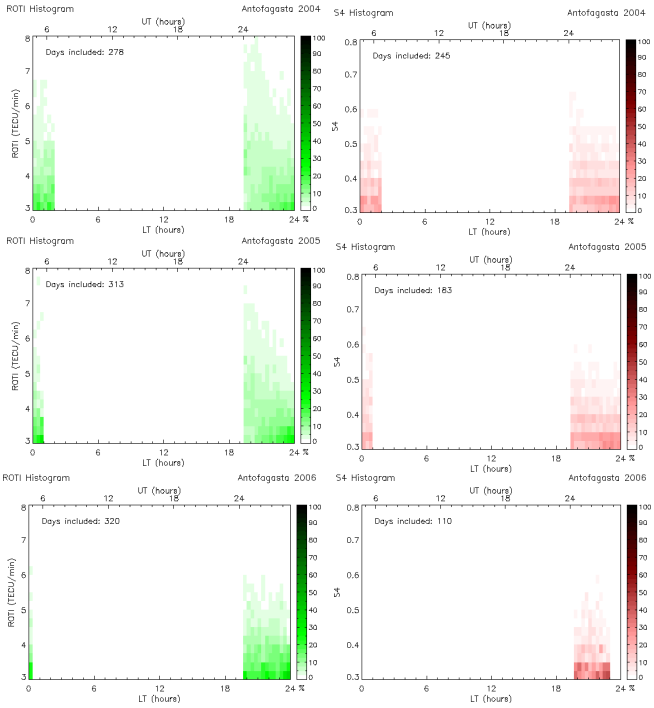

Figure 7. Annual histograms of fast ROTI (left) and S_4 (right) for the years 2004 - 2006 at Antofagasta, Chile.

We also examined the statistical behavior of TEC fluctuations and scintillation activity as a function of magnetic latitude. Figure 8 shows annual histograms of fast ROTI and S_4 in 2006 for ground stations with magnetic latitudes of 3° N, 6° S, and 16° S. Once again, it was observed that the onset and duration of TEC fluctuations, as characterized by fast ROTI, approximately coincide with scintillation activity at the GPS L1 frequency. Both TEC fluctuations and scintillation are observed to be stronger for stations near the anomaly crests than near the magnetic equator.

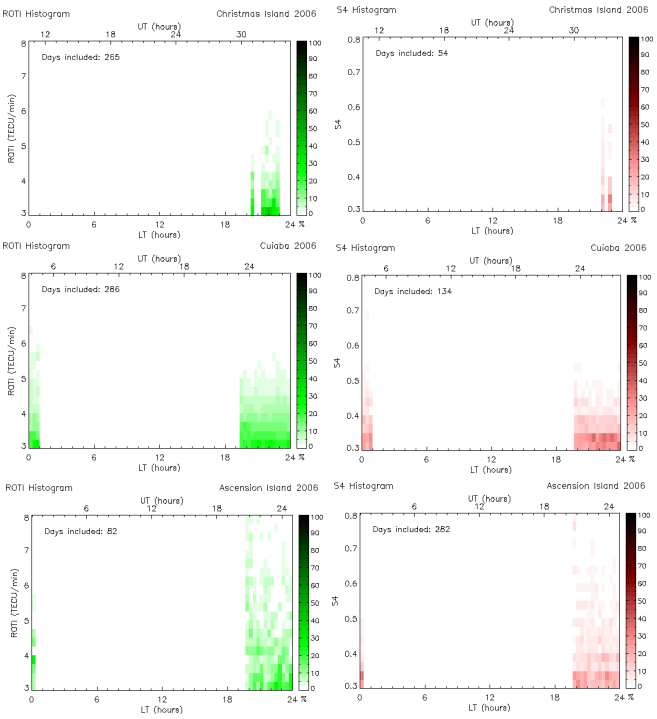

Figure 8. Annual histograms of fast ROTI (left) and S_4 (right) in 2006 at Christmas Island, Cuiaba, and Ascension Island with magnetic latitudes of 3° N, 6° S, and 16° S, respectively.

CONCLUSIONS

Large scale TEC gradients and small scale TEC fluctuations in the low latitude ionosphere result from a number of physical mechanisms. These include variations in the development of the Appleton anomaly, geomagnetic activity, plasma turbulence due to equatorial spread F, and solar flux variations among others. By generating annual histograms of TEC, fast ROTI, and S_4 using measurements collected by the dual frequency GPS

receivers of the AFRL-SCINDA network, we are able to make a few general observations about the statistical behavior of TEC variations in the low latitude ionosphere as a function of local time, magnetic latitude, and solar flux.

The magnitude and variability of TEC measured by GPS receivers in the low latitude region increase substantially with proximity to the crests of the Appleton anomaly. Both the magnitude and variability of TEC also increase with increasing solar flux (as solar maximum conditions are approached). We found the onset and duration of TEC fluctuations, as characterized by the fast ROTI parameter, approximately coincides with the onset and duration of scintillation activity at the GPS L1 frequency on a statistical basis. Both TEC fluctuations and scintillation activity are more intense near the crests of the anomaly and as conditions approach those of solar maximum.

These results indicate that, at least in the cases examined, the fast ROTI parameter may be used as a proxy for scintillation activity at the L1 frequency. We believe the correlation of these two parameters is largely due to two factors. First, we have selected a sufficiently fast sampling rate for evaluating ROTI to ensure that it is sensitive to irregularities smaller than the Fresnel scale which can contribute to scintillation at the L1 frequency. Second, the variance of TEC fluctuations appears in the definition of fast ROTI and also in a related way, as electron density fluctuations along the propagation path, in the formulation the phase screen theory. As such, fast ROTI may be thought of as crude proxy for a phase screen, although this interpretation would perhaps be clearer if we had detrended the TEC (so that only the TEC fluctuations were allowed to contribute) prior to using it to compute fast ROTI. In any case, the phase screen description depends on a host of other parameters such as the **E**x**B** drift velocity, the spectrum of irregularities, and the anisotropy of the irregularities which are not reflected in the fast ROTI parameter. Hence a universally applicable relationship between fast ROTI and S_4 is unlikely to be found. Also, noise in the TEC is amplified when calculating its rate of change, which can prevent its effective use as an indicator of scintillation activity if the fluctuations that contribute to scintillation are buried in the receiver oscillator noise. Nevertheless, the results from this study suggest that fast ROTI can provide a useful indicator of scintillation activity at the GPS L1 frequency, at least on a statistical basis.

ACKNOWLEDGMENTS

This work was supported by AFRL contract FA8718-06-C-0022.

REFERENCES

Basu, S., K. Groves, J. Quinn, and P. Doherty, A comparison of TEC fluctuations and scintillations at Ascension Island, *J. Atmos. Terr. Phys.*, 61, 1219, 1999.

Beach, T., and P. Kintner, Simultaneous global positioning system observations of equatorial scintillations and total electron content fluctuations, *J. Geophys. Res.*, 104, 22553, 1999.

Carrano, C., GPS-SCINDA: a real-time GPS data acquisition and ionospheric analysis system for SCINDA, submitted for publication as an AFRL technical report, 2007.

Carrano, C., and K. Groves, The GPS segment of the AFRL-SCINDA global network and the challenges of real-time TEC estimation in the equatorial ionosphere, Proceedings of the Institute of Navigation, National Technical Meeting, Monterey, CA, 2006.

Groves, K., S. Basu, E. Weber, M. Smitham, H. Kuenzler, C. Valladares, R. Sheehan, E. MacKenzie, J. Secan, P. Ning, W. McNeil, D. Moonan, and M. Kendra, Equatorial scintillation and systems support, *Radio Sci.,* 32, 2047, 1997.

Henderson, S., Swenson, C., Christensen A., and Paxton, L., Morphology of the equatorial anomaly and equatorial plasma bubbles using image subspace analysis of Global Ultraviolet Imager data, *J. Geophys. Res.*, 110, doi: 10.1029/2005JA011080, 2005.

Rino, C., A power law phase screen model for ionospheric scintillation, 1. weak scatter, *Radio Sci.,* 14, 1135, 1979.